DESIGN AND EXPERIMENT OF PRECISION SEED METERING PLATE FOR EDIBLE SUNFLOOWER BY ADDING SEED GUIDE BAR

/

增加导种条式食葵精量排种盘设计及试验

Fengli LI[1], Jianghui CHEN[1], Keyi LIU[1], Jia ZHANG[1], Yaou ZHANG[1], Junchi YIN[1], Fei LIU[2], Manquan ZHAO [*2]

[1]College of Mechanical and Electrical Engineering, Xinjiang Institute of Engineering, Urumqi 830023, China;

[2]College of Mechanical and Electrical Engineering, Inner Mongolia Agricultural University, Hohhot 010018, China;

Tel: +86 13139630536; E-mail: lifid@126.com

DOI: https://doi.org/10.35633/inmateh-72-15

Keywords: *air suction metering device, edible sunflower, adsorption stance, high-speed camera technology, seeding performance*

ABSTRACT

In order to solve the problems of easy seed shedding and poor seed population mobility during sowing, a precision seed metering tray for edible sunflowers with seed guide strips was designed in this paper. This article aims to adjust the adsorption posture of sunflower seeds by designing three types of structures: triangular seed guide strip, rectangular seed guide strip, and diamond seed guide strip. Seed population motion simulation and seeding performance experiments were conducted on the seeder. The experimental results show that adding a triangular seed guide strip to the seeding tray has the best disturbance effect on the seed population, with the highest proportion of seeds in the first adsorption stance seed (the seed centroid was adsorbed) and the highest qualification index. The working parameters for the best seed metering performance were obtained: the rotating speed of the seed metering disc was 8.41 r/min, and the vacuum degree was 3.5 kPa.

摘要

为提高气吸式食葵排种器的排种性能，解决播种过程中种子易脱落、种群流动性差等问题，本文以调整食葵种子的吸附姿态为切入点，对气吸式排种器排种盘进行了设计改进，设计了三角形导种条、矩形导种条、菱形导种条 3 种结构，并对排种器进行了种群运动仿真和排种性能试验。试验结果表明，增加三角形导种条的排种盘，对种群扰动效果最好，姿态一（种子质心被吸附）种子比例最高，合格指数最高。得到三角形导种条排种盘排种性能最佳时的工作参数：排种盘转速 8.41 r/min，真空度 3.5 kPa。

INTRODUCTION

As an important cash crop in China, edible sunflower cultivation is an important link in its production process. The air-suction seed metering device has low requirements for seed shape, strong adaptability, and good versatility, especially for seeds with irregular shapes. However, for seeds with large sizes and irregular shapes, it needs to have good mobility in the seed chamber.

Some studies have improved the seeding performance of seeds by improving the structure of the seeding tray (*Sun et al., 2020; Ye et al., 2021; Zhang et al., 2021; Dylan et al., 2013; Yazgi et al., 2014; Neto et al., 2012; Khobragade et al., 2012; Karael, 2009*). Electronically controlled seed singulation devices was being studied (*Cristian et al., 2015*). Onal et al used CFD software to simulate the seeding process of the metering device and analyzed the velocity and pressure fields of the rice bud seeds during the filling process (*Onal et al., 2012*).

Some studies used EDEM software to simulate seed population motion (*Tijskens et al., 2003*) and analyze the impact of working parameters on seed population motion (*Zhu et al., 2023; Wang et al., 2023; Dong et al., 2022*). Because increasing seed population mobility in the seed filling area can help improve seed filling performance, some scholars have designed and improved the seeding tray to increase population mobility in the seed filling area. It was verified the conclusion that improving the seeding tray can improve seed population mobility by using EDEM software to simulate population movement (*Wang et al., 2021; Boac et al., 2010; Zhang et al., 2021; Min et al., 2017*). Some scholars also used EDEM software to simulate and analyze the filling performance of seeds (*John et al., 2018; Lysych et al., 2023*).

Recently, some domestic and foreign scholars have used the coupling method of Discrete Element Method (DEM) and Computational Fluid Dynamics (CFD) to simulate the working process of an air suction seeder and analyze relevant parameters, such as the seed motion in the airflow field (*Han et al., 2018*).

In summary, the scholars mentioned above have conducted in-depth research on the flow of seeds in the seed chamber during the air suction seed metering process and achieved good results. However, there are few reports on edible sunflowers' fluidity and adsorption stance in the air suction seeder chamber. According to previous research (*Li et al., 2018*), there are three main adsorption stances when suction holes adsorb edible sunflower seeds. The first adsorption stance is that the seed centroid is adsorbed; The second adsorption stance is that one end of the seed is adsorbed; The third adsorption stance is that the tip of the seed is sucked into the suction hole. And the first adsorption stance is relatively stable. As well as the higher the proportion, the better the seeding performance. This article took the 2BM-5 air suction seeder as the research object to study the adsorption stability of seeds with different adsorption stances. The ultimate goal is to improve the seeding performance of the air suction seeder by improving the structure of the seeding tray, discrete element simulation, and indoor experiments.

MATERIALS AND METHODS

COMPOSITION AND WORKING PRINCIPLE OF THE AIR-SUCTION PRECISION METERING DEVICE

The air-suction precision metering device is shown in Fig.1. The working principle of the air-suction precision metering device is as follows: the seed metering disc separates the vacuum chamber from the seed chamber. Moreover, the vacuum chamber is connected to the fan through a hose. When the fan is working, the vacuum chamber generates negative pressure. Then, the suction force is formed at the suction hole of the seed tray, which adsorbs the seeds in the seed chamber. The seeds rotate along with the seeding tray to the seeding area. Because the pressure in the vacuum chamber disappears, all seeds are seeded under the action of gravity.

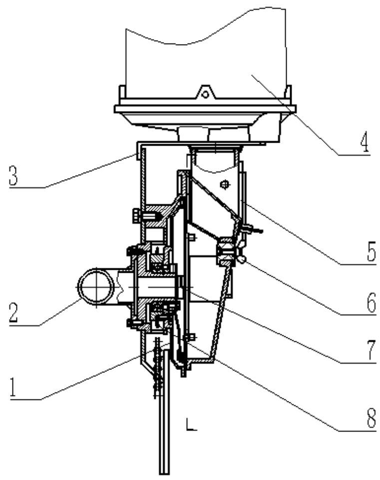

Fig. 1 - Structure of the air suction seed metering device

1- Vacuum chamber; 2- Inlet pipe; 3- Seed metering housing; 4- Seedbox; 5- Seed storage device; 6- Limit plate; 7- Seed metering disc; 8- Seed metering sprocket

DESIGN AND ANALYSIS OF PLANTER PLATE STRUCTURE

Seed sizes of edible sunflower and parameters of planter plate

Randomly selected 100 confectionery edible sunflower seeds and measured their length (L), width (W), and thickness (H) using a vernier caliper with an accuracy of 0.02 mm (Fig. 2). The average of the experimental results shows that the length, width, and thickness of confectionery edible sunflower seeds are 16.11, 7.6, and 4.29 mm, respectively.

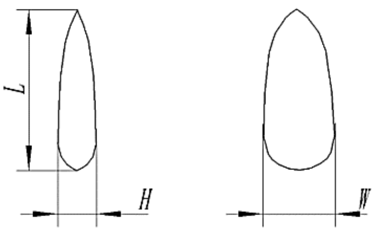

Fig. 2 - Diagram of the triaxial size of edible sunflower seed

The basic parameters of the planter plate are as follows: diameter is 200 mm, thickness is 2 mm, rotation radius of the suction hole center is 82.5 mm, and suction hole diameter is 5 mm (Fig. 3).

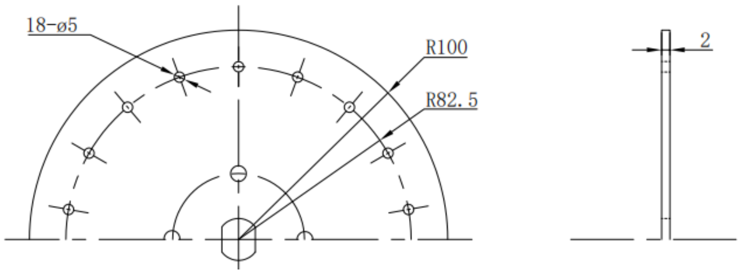

Fig. 3 - Schematic diagram of the planter plate structure

The structure design of the planter plate

As shown in Fig. 4, the seed guide strip is evenly arranged along the circumference of the outer tangent circle of the suction hole. Its one side is perpendicular to the connector of the center of the seeding disc and the center of the suction hole. At the same time, it is tangent to the suction hole, with the tangent point being the midpoint of this edge. An isosceles triangle is selected as the shape of the seed guide strip, with a bottom edge of 8 mm. The longer the seed guide strip length, the more obvious the stirring effect on the seeds. Therefore, the length of L_s of the seed guide strip should be greater than the average length of the seeds.

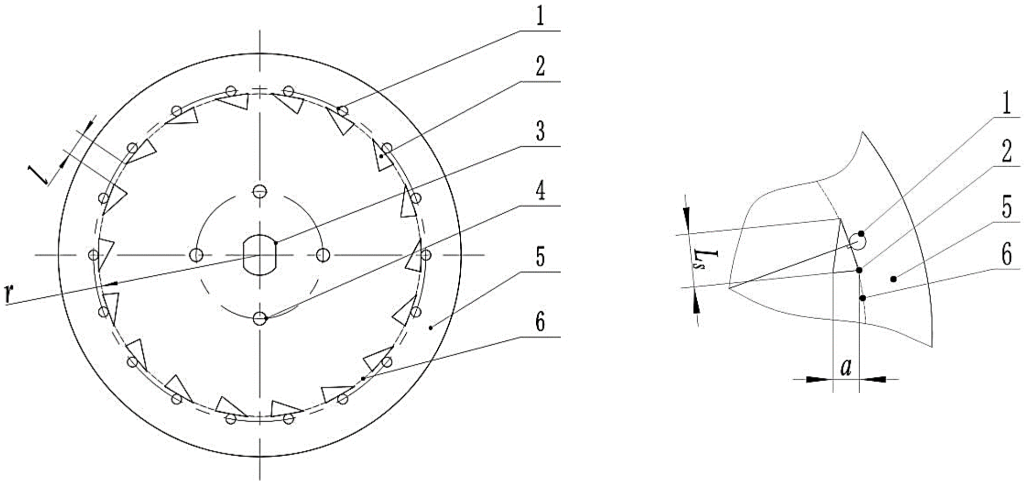

Fig. 4 - Arrangement position of triangle guide strip

1- Suction hole; 2- Triangle seed guide; 3- Power transmission hole; 4- Installation hole; 5- Seed tray; 6- The circle on the inner side of the suction hole edge line

However, the size of the seed chamber must be considered, as well as the distance l between the two seed guide strips. If l is too small, it is easy to grip the seeds. Hence, l should be greater than or equal to $\frac{L}{2}$. The length of the seed guide strip is as follows:

$$\mathrm{L} \leq \mathrm{L_S} \leq \frac{1}{9}\pi\mathrm{r} - \frac{\mathrm{L}}{2} \tag{1}$$

In Eq.(1), L_S is the height of the triangular seed guide strip, mm; r is the radius of the circle tangent to the suction hole, mm. To prevent excess seeds from being adsorbed by suction holes and difficult to fall off, as well as to carry excess seeds to the seed feeding area during the rotation of the seeding disc, its thickness is as follows:

$$\mathrm{H_S} \leq \mathrm{H} \tag{2}$$

In Eq.(2), $\mathrm{H_S}$ is the thickness of the triangular seed guide strip, mm. The final length and thickness of the seed guide strip were determined to be 18 mm and 2 mm.

As shown in Fig. 5, the center line of the length direction of the seed guide strip coincides with the line connecting the center of the suction hole and the center of the seeding disc, and the short side of the rectangle is tangent to the suction hole. Considering the size of the seed mixing wheel and seed chamber, the length L_j of the rectangular seed guide strip is 12 mm. The width W_j of the seed guide strip is designed based on the seed width, which is 6 mm.

To prevent the seed guide strip from carrying the seeds to the seeding area when the seeding disc rotates, the thickness of the guide strip is 2 mm. The seed guide strip was chamfered to enhance the fluidity of the seeds at the suction hole.

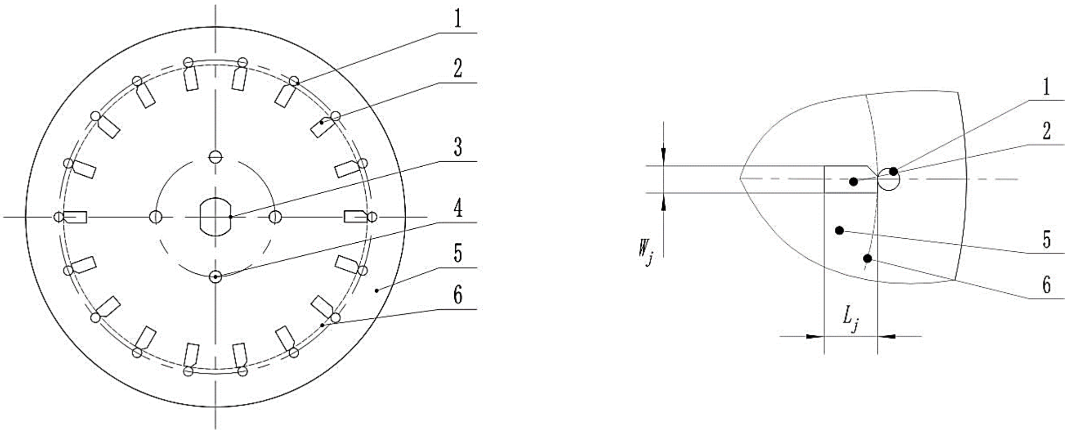

Fig. 5 - Arrangement position of the rectangle guide strip

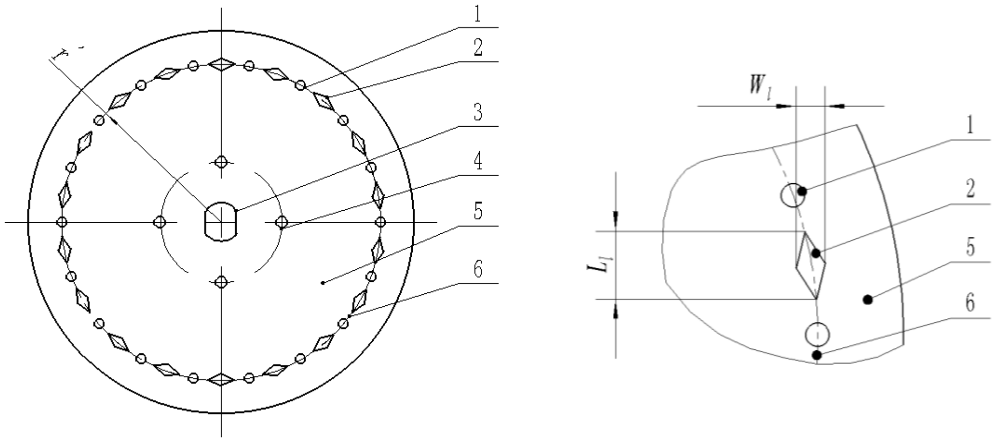

Fig. 6 - Arrangement position of the rhombus guide strip

The length direction of the diamond-shaped seed guide strip is evenly arranged along the circle where the center of the suction hole is located. Also, the seed guide strip is located in the middle of the two suction holes. The arrangement diagram is shown in Fig.6. W_l is similar to the seed width, which is 6 mm. Then, the thickness is 2 mm. The length of the seed guide strip is as follows:

$$L_l \leq \frac{1}{9}\pi r' - L \tag{3}$$

In Eq.(3), r' is the radius of the circle where the center of the suction hole is located, mm; L_l is the length of the diamond shaped seed guide strip, mm. L_l is determined as 14 mm. The dimensions of three kinds guide bars are shown in Fig. 7.

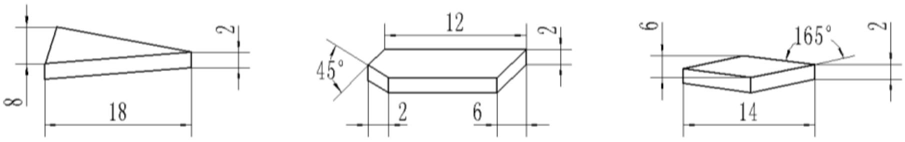

Fig. 7 - The sizes for seed guide strips

Force analysis of the seed on the seed guide strip

Due to the same force situation on the triangular and rectangular seed guide strips during the seed carrying process, the seed on the triangular seed guide strips was analyzed as the object (Fig.8). It is assumed that all external forces act on the centroid of the seed, with the seed centroid as the origin o. The rotation direction of the seeding disk was the *oi* direction. The *Oj* direction was the direction from the center of mass points to the center of the seeding disc. Moreover, the direction perpendicular to the plane of the seeding disk was the *ok* direction. Finally, a natural coordinate system was established. If the seed did not roll, there must be:

$$(F_S' - N_k)\frac{d}{2} = Q_1\frac{H}{2} \tag{4}$$

In Eq.(4), Q_1 is the combined force of G, F_e, N_3, F_3, F_{2j} and F_{2i} , N; F_S' is the suction force on the seed on the seed guide strip, N; N_3 is the binding force of the seed guide strip on the seed, N; F_3 is the frictional force between the seed and the seed guide strip, $F_3 = f_3 N_3$; f_3 is the friction coefficient between the seed guide and the seed; F_{2i} is the component of the frictional force between the seed and the seeding disc in the oi direction, N; F_{2j} is the component of the frictional force between the seed and the seeding disc in the oj direction, N; G is the gravity of the seed, N; F_e is the inertial force involved, N; N_k is the binding force of the suction hole on the seed, N, d is the diameter of the suction hole, mm.

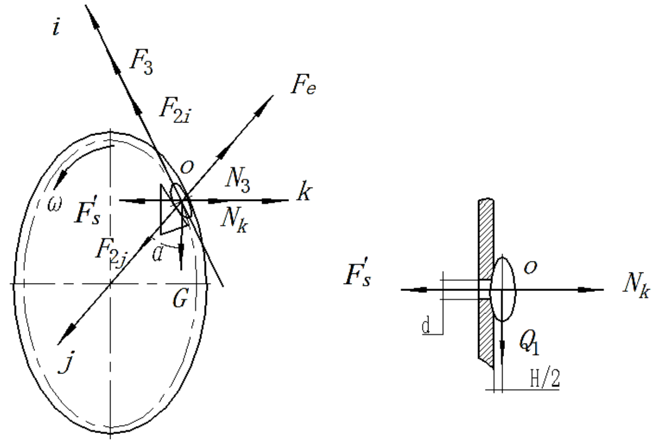

Fig. 8 - Stress analysis of the critical state of seed adsorption

When $N_k = 0$, it is the critical state for seed adsorption, where:

$$F_S' \frac{d}{2} = Q_1 \frac{H}{2} \tag{5}$$

In Eq. (5), $F_S' = P_1' \frac{\pi d^2}{4}$,$Q_1 = \sqrt{(F_3 - G\sin\alpha)^2 + (G\cos\alpha - F_e - N_3)^2}$, $P_1'$is the critical adsorption vacuum of the suction chamber when the seed on the seed guide strip does not roll, kPa.

Each force is introduced into Eq.(5), then it can be obtained:

$$P_1' = \frac{4H}{\pi d^3}\sqrt{(F_3 - G\sin\alpha)^2 + (G\cos\alpha - F_e - N_3)^2} \tag{6}$$

According to previous research (*Li et al., 2018*), the non-rolling critical vacuum degree of the adsorbed seed for the first adsorption stance during the seed-carrying process without a guide strip is:

$$P_1'' = \frac{4H}{\pi d^3}\sqrt{G^2\sin^2\alpha + (G\cos\alpha - F_e)^2} \tag{7}$$

Due to $F_3 < N_e$, the comparison between equations (6) and (7), it can be seen that $P_1' < P_1''$. Therefore, adding triangular and rectangular seed guide strips on the seeding tray can reduce the vacuum degree of seed carrying. Under the same vacuum degree, adding triangular and rectangular seed guide strips will result in a more stable seed state adsorbed.

SEED MOTION SIMULATION

This paper analyzes the seed motion simulation through discrete element software. The purpose is to explore the disturbance effect of different structure seed guides on the seeds.

Set global variable parameters

The surface of sunflower seeds is smooth without adhesion, and Hertz Mindlin (no slip) is selected as the simulation contact model. The other parameters are shown in Tab. 1.

Table 1

Global variable parameter setting

Item	Property	Value
Edible sunflower	Poisson's ratio	0.35
	Shear modulus/MPa	26.73
	Density/kg·m^{-3}	476.92

Item	Property	Value
Seed plate	Poisson's ratio	0.3
	Shear modulus/MPa	70000
	Density/kg·m^{-3}	7800
Seed chamber	Poisson's ratio	0.5
	Shear modulus/MPa	35
	Density/kg·m^{-3}	1180
Seed stirring device	Poisson's ratio	0.39
	Shear modulus/MPa	71.94
	Density/kg·m^{-3}	1050
Edible sunflower-edible sunflower	Static friction coefficient	0.34
	Dynamic friction coefficient	0.12
	Impact recovery factor	0.42
Edible sunflower-seed plate	Static friction coefficient	0.43
	Dynamic friction coefficient	0.1
	Impact recovery factor	0.51
Edible sunflower-seed chamber	Static friction coefficient	0.45
	Dynamic friction coefficient	0.19
	Impact recovery factor	0.49
Edible sunflower-seed stirring device	Static friction coefficient	0.43
	Dynamic friction coefficient	0.14
	Impact recovery factor	0.48

Establishment of the model for edible sunflower

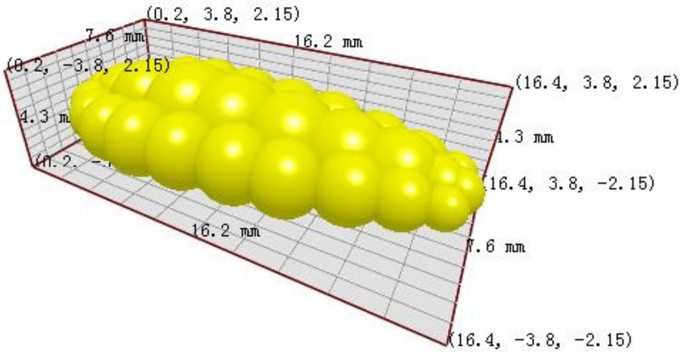

Fig. 9 - The seed model of edible sunflower

When establishing the edible sunflower seed model, adjust the length, width, and thickness of the seed model to 16.2 mm, 7.6 mm, and 4.3mm, respectively. The seed model is composed of 30 balls, as shown in Fig.9.

Establishment of the seeder model

The simplified air suction precision seeder consisted of three parts: seed chamber, seed tray, and seed stirring device (including seed stirring wheel and guide strips). The variable parameters of these three parts were set according to Table 1. The particle factory was built on the upper part of the seed chamber of the seeder, and the total number of particles was 2000. The simulation time step was 2.6 × 10^{-6} seconds. The total simulation time was 8 seconds, and the output time step was 0.05 seconds. The working conditions of the seeder during simulation were set as follows: the amplitude in the y-direction was 3 mm, and the vibration frequency was 5 Hz; The rotation speed of the seeding disc and the stirring wheel was 8.41 r/min. The starting time for vibration and rotation was 1.2 seconds. The seeder began to operate when all seeds were generated by the particle factory and the population motion state was stable.

RESULTS

SEED MOTION SIMULATION EXPERIMENT AND RESULT ANALYSIS

Test design

The impact of seed guide strips on seed disturbance was studied. Then, non-seed guide strips (disc A), triangular seed guide strips (disc B), rectangular seed guide strips (disc C), and diamond seed guide strips (disc D) were selected as experimental factors. These seeds in the suction area next to the seeding tray were chosen as the research object (Fig.10). The disturbance effect of different seed guides on seeds was evaluated with the average velocity and displacement in the y direction of the seeds. Using the post-processing function of EDEM software, the y-direction average velocity and average displacement of the seed population within the simulation time of 1.2-8 seconds were output.

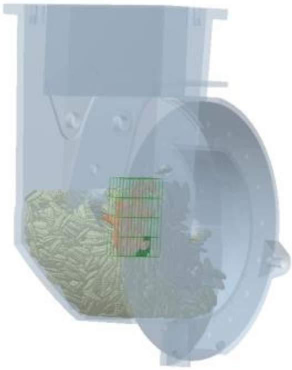

Fig. 10 - Seed absorption area position

Test results and analysis

Test results are shown in Table 2. The average velocity and displacement in the y-direction of disc B, C and D are improved. Therefore, with the addition of seed guide strips, the disturbance effect of the seed population in the suction hole area is strengthened. Among them, disk B has the best disturbance effect.

Table 2

Average velocity and displacement in the y-direction of the seed population

Seed plate	Average velocity in y direction/(m/s)	Average displacement in y direction/mm
Disc A	0.008	1.51
Disc B	0.017	3.16
Disc C	0.015	3.01
Disc D	0.009	2.17

SEED METERING PERFORMANCE TEST AND RESULT ANALYSIS

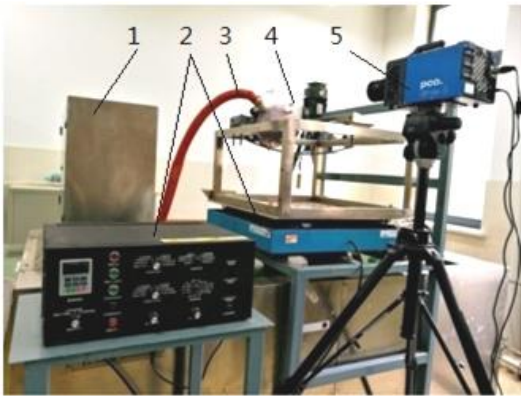

Fig. 11 - Arrangement position of triangle guide strip

1- JPS-12 type seed metering performance test-bed; 2- Suction electromagnetic vibration table; 3- Pneumatic system; 4- Suction seed metering device; 5- High speed camera

As shown in Fig. 11, the seeding performance test was conducted on the JPS-12 seeding performance detection test bench, and the high-speed camera is placed in front of the seeding device to capture and record the seeding process.

Single factor seeding performance test and result analysis

Test design

As shown in Fig.12, the structural parameters of the seed guide strip were selected as experimental factors, and the seeding performance and the seed adsorption stance were evaluated as evaluation indicators for single factor seeding performance test. The working parameters during the experiment were as follows: The speed of the seeding disc was 8.41 r/min. The vacuum degree was 3.5 kPa. The amplitude of the seeding device was 3 mm. The height of the seeding layer was 60 mm. Each group of experiments was repeated three times, and 250 particle pitches were taken for each experiment when the test bench was running smoothly and the corresponding seed adsorption stances were recorded.

a. Disc A *b. Disc B* *c. Disc C* *d. Disc D*

Fig. 12 - Four different types of planter plates of edible sunflower

Test results and analysis

As shown in Table 3, the proportion of the first adsorption stance is increased for disk B, C and D, while the proportion of the second adsorption stance and the third adsorption stance are decreased. The seed adsorption stance of disc B is the best.

Table 3

Effect of each planter plate on the adsorption stance of edible sunflower seeds

Type of seed metering tray	The first adsorption stance/%	The second adsorption stance/%	The third adsorption stance/%	No stance/%
Disc A	71.36	12.39	10.24	6.01
Disc B	87.74	1.11	8.04	3.11
Disc C	76.7	8.16	9.01	6.13
Disc D	74.6	10.16	9.73	5.51

As shown in Table 4, the qualified index of disc B, C and D is increased, while the repeat index sowing and leak index are decreased. Among them, the qualified index is highest for disc B, while the repeat sowing index and leak index are the lowest.

Table 4

Seeding performance of each planter plate in edible sunflower

Type of seed metering tray	Qualified index (%)	Repeat sowing index (%)	Leak index (%)
Disc A	79.21	14.78	6.01
Disc B	91.57	5.32	3.11
Disc C	84.03	10.68	5.29
Disc D	80.78	13.71	5.51

Dual factor seeding performance test and result analysis

Test design

Through single-factor experiments, it was determined that disc B was more suitable for sowing edible sunflowers, so disc B was selected as the experimental object. A dual-factor seeding performance test was conducted. The rotation speed of the seeding disc and vacuum degree were used as experimental factors. Then, the seeding performance and the seed adsorption stance were recorded. The level of experimental factors is shown in Table 5. Each group of experiments was repeated three times, and 250 particle pitches were taken for each experiment when the test bench ran smoothly. The corresponding seed adsorption stances were taken notes.

Table 5

Test factor level of edible sunflower

Factor	Level				
	1	2	3	4	5
The planter plate speed / (r/min)	6.29	7.35	8.41	9.47	10.53
Vacuum degree / kPa	2.3	2.9	3.5	4.1	4.7

Test results and analysis

The average value of three repeated experiments was taken as the experimental result. The surface graph is shown in Fig. 13. As the rotational speed increases, the qualified index shows an up-down trend, it is the highest with a vacuum degree of 3.5 kPa and a rotation speed of 8.41 r/min. Except for the vacuum degree of 4.7 kPa, the repeat sowing index under all other vacuum degrees showed a downward trend, it is the lowest with a vacuum degree of 2.3 kPa and a rotation speed of 10.53 r/min. The leak index shows an upward trend, it is the lowest with a vacuum degree of 4.7 kPa and a rotation speed of 6.29 r/min. The proportion of the first adsorption stance shows an up-down trend, it is the highest with a vacuum degree of 3.5 kPa and a rotation speed of 8.41 r/min. The change trend of the proportion of the second adsorption stance is not apparent, it is the lowest with a vacuum degree of 3.5 kPa and a rotation speed of 8.41 r/min. When the vacuum degree is 2.3 kPa and 4.7 kPa, the proportion of the third adsorption stance shows a downward trend, while under other vacuum degrees, it shows a down-up trend. It is the lowest with a vacuum degree of 2.3 kPa and a rotation speed of 10.53 r/min. The optimal working parameters for planting edible sunflowers reasonably and densely are a vacuum degree of 3.5 kPa and a rotation speed of the seeding disc of 8.41 r/min.

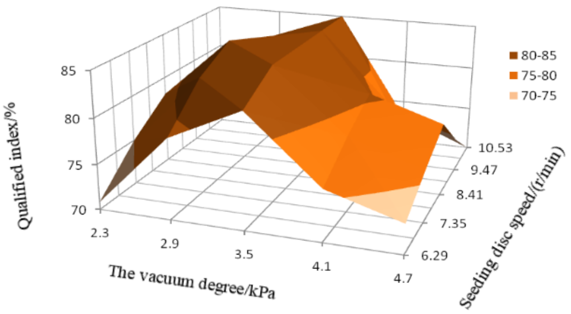

a. Qualified index

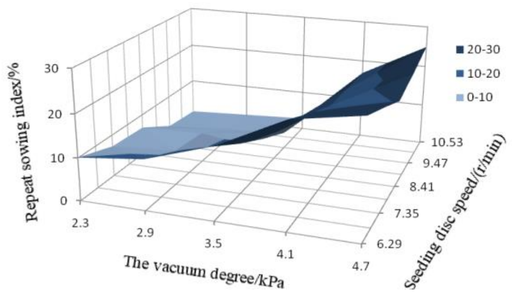

b. Repeat sowing index

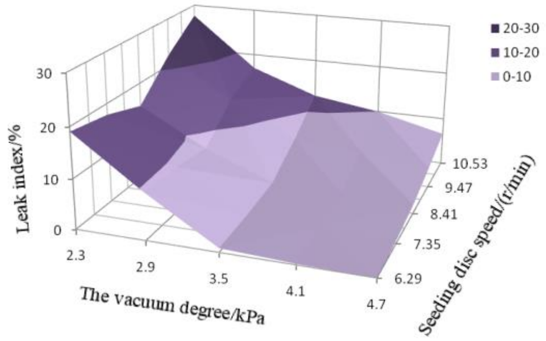

c. Leak index

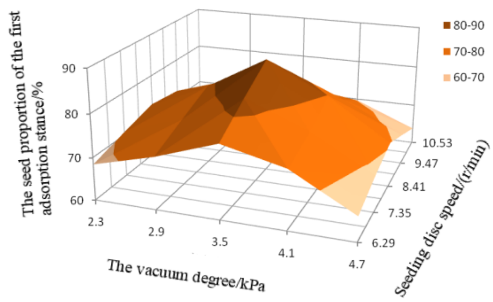

d. The seed proportion of the first adsorption stance

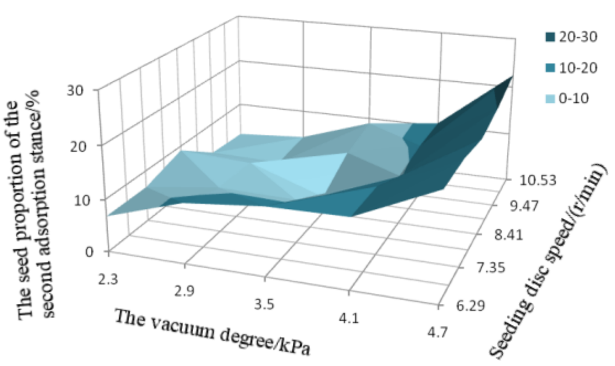

e. The seed proportion of the second adsorption stance

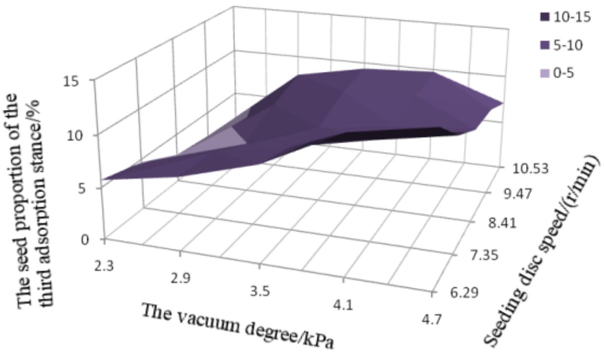

f. The seed proportion of the third adsorption stance

Fig. 13 - The influence surface graph of the seeding performance and adsorption stance

CONCLUSIONS

In this paper, three types of seed guide strip structures were designed. By analyzing the force on the seeds on the guide strip, adding triangular and rectangular guide strips can reduce the vacuum degree of seed carrying. By simulating and analyzing the seed population movement, it can be seen that the average velocity and displacement in the y-direction of disc B, C and D have increased. Therefore, the disturbance effect on the seed population in the suction hole area was enhanced by adding guide strips. A single-factor seeding performance test was conducted. It can be obtained that the seed adsorption stances were adjusted for disc B, C and D. In these three types of seeding trays, the proportion of the first adsorption stance for seeds was increased. Disc B has the highest proportion of the first adsorption stance for seeds and the best seeding performance. The dual factor seeding performance test was carried out, and the best working parameters were obtained. The effect of the improved seeding tray on the seeding performance of Mengjichang 3638C sunflower seeds was studied in this paper. However, there is a wide variety of edible sunflower seeds, and the shape and position of the seed guide need to be optimized and improved.

ACKNOWLEDGEMENT

The supports of the Natural Science Foundation of Xinjiang Uygur Autonomous Region (2022D01B19) and Doctoral Research Initiation Fund Project of Xinjiang Institute of Engineering (2020xgy042302) for this research are greatly appreciated.

REFERENCES

[1] Boac, J.M., Casada, M.E., Maghiang R.G., et al, (2010). Material and interaction properties of selected grains and oilseeds for modeling discrete particles, *Transactions of the ASABE*: 53(4):1201-1216.

[2] Cristian I., Octavian P. (2015). A New Concept for Seed Precision Planting. *Agriculture and Agricultural Science Procedia*, 6:38-43.

[3] Dong X.Q., Zheng H.N., Jia X., et al, (2022), Calibration and experiments of the discrete element simulation parameters for rice bud damage. *INMATEH-Agricultural Engineering*, 68(3):659-668.

[4] Dylan S., J., Dianne C.H., Andrew L.G., (2013), Precision metering of Santalum spicatum (Australian Sandalwood) seeds, *Biosystems Engineering*,115(2):171-183.

[5] Han D.D., Zhang D.X., Jing H.R. et al, (2018), DEM-CFD coupling simulation and optimization of an inside-filling air-blowing maize precision seed-metering device. *Computers and Electronics in Agriculture*, 150: 426-438.

[6] John M.T., Wang D.C., Ma W.P. et al, (2018), Design and optimization of the vertical plate metering device for alfalfa seeds precision based on engineering discrete element method (EDEM). *Innovative Systems Design and Engineering*, 9(6): 16-22.

[7] Karael D. (2009), Performance of a modified precision vacuum seeder for no-till sowing of maize and soybean. *Soil and Tillage Research*, 104(1) :121-125.

[8] Khobragade H.M., Kamble A.K., Dave A.K. (2012), Performance evaluation of pneumatic seed metering device for paddy in puddle. *International Journal of Agricultural Engineering*，5(1) : 98-102.

[9] Li F.L., Chen J.H., Liu F. et al, (2018), Influence of seed adsorption stance on seeding performance based on high speed camera technology (*基于高速摄像技术种子吸附姿态对排种性能的影响*) *Journal of China Agricultural University*, 23(4): 128-136.

[10] Lysych M.N., Chernyshev V.V., Nagaytsev V.M., (2021), Design and simulation of seed metering device for aero sowing of forest pelleted seeds. *International Conference on IT in Business and Industry*, 2032: 1-7.

[11] Min S.W., Dooyum D.U., Sang M.S., et al, (2017), Development of seeder for mixed planting of corn and soybeans, *International Journal of Agricultural and Biological Engineering*,10(3):95-101.

[12] Neto W.H.P., Justino A., Namur T.R., et al, (2012), Comparison of metering mechanisms of corn seed (Comparação entre mecanismos dosadores de sementes demilho), *Engenharia Agrícola*, 32(5):981-988.

[13] Onal I., Degirjviencioglu A., Yazgi A., (2012), An evaluation of seed spacing accuracy of a vacuum type precision metering unit based on theoretical considerations and experiments, *Turkish Journal of Agriculture Forestry*, 36(2):133-144.

[14] Sun D., Cui Q.L., Zhang Y.Q., et al, (2020), Performance test of the 2BDE-2 type millet fine and small-amount electric seeder. *INMATEH-Agricultural Engineering*, 60(1):129-136.

[15] Tijskens E, Ramon H, Baerdemaeker J D. (2003). Discrete element modelling for process simulation in agriculture. *Journal of Sound and Vibration*, 266:493-514.
[16] Wang Y.B., Li H.W., Wang Q.J., et al, (2021), Experiment and parameters optimization of seed distributor of mechanical wheat shooting seed-metering device. *INMATEH-Agricultural Engineering*, 63(1):29-40.
[17] Wang Y.C., Kang X.Q., Wang G.Q., et al, (2023), Numerical analysis of friction-filling performance of friction-type vertical disc precision seed-metering device based on EDEM. *Agriculture*,13(12):2183
[18] Yazgi A., Degirmencioglu A., (2014), Measurement of seed spacing uniformity performance of a precision metering unit as function of the number of holes on vacuum plate, *Measurement*, 56:128-135.
[19] Ye S.B., Zheng D.C., Li W., et al, (2021), Design and test of negative pressure chamber rotary buckwheat seed metering device. *INMATEH-Agricultural Engineering*, 64(2):185-194.
[20] Zhu H.B., Wu X., Bai L.Z., et al, (2023), Design and experiment of a soybean shaftless spiral seed discharge and seed delivery device. *Scientific Reports*, 13(1):20751-20751.
[21] Zhang K.X., Zhang L., Ding Y. et al, (2021), Design and test of air-suction pepper seed metering device based on air supply and quantitative seed supply, *INMATEH-Agricultural Engineering*, 64(2):345-354.
[22] Zhang X.S., Zhu D.Q., Xue K., et al, (2021), Parameter optimization and experiment of slider-hole-wheel seed-metering device based on discrete element method, *INMATEH-Agricultural Engineering*, 65(3):410-420.